Metrol. Meas. Syst., Vol. 29 (2022) No. 1, pp. 191–205
DOI: 10.24425/mms.2022.138541

METROLOGY AND MEASUREMENT SYSTEMS
Index 330930, ISSN 0860-8229
www.metrology.wat.edu.pl

DIAGNOSIS OF MULTIPLE FAULTS OF AN INDUCTION MOTOR BASED ON HILBERT ENVELOPE ANALYSIS

Ahmet Kabul[1)], Abdurrahman Ünsal[2)]

1) *Burdur Mehmet Akif Ersoy University, Department of Electrical and Electronic Engineering, 15030, Burdur, Turkey* (✉ *ahmetkabul@mehmetakif.edu.tr*, +90 248 213 2761)
2) *Kütahya Dumlupınar University, Department of Electrical and Electronic Engineering, 43100, Kütahya, Turkey* (*unsal@dpu.edu.tr*)

Abstract

Three phase induction motors are widely used in industrial processes and condition monitoring of these motors is especially important. Broken rotor bars, eccentricity and bearing faults are the most common types of faults of induction motors. Stator current and/or vibration signals are mostly preferred for the monitoring and detection of these faults. Fourier Transform (FT) based detection methods analyse the characteristic harmonic components of stator current and vibration signals for feature extraction. Several types of simultaneous faults of induction motors may produce characteristic harmonic components at the same frequency (with varying amplitudes). Therefore, detection of multiple faults is more difficult than detection of a single fault with FT based diagnosis methods. This paper proposes an alternative approach to detect simultaneous multiple faults including broken rotor bars, static eccentricity and outer/inner-race bearing faults by analysing stator current and vibration signals. The proposed method uses Hilbert envelope analysis with a Normalized Least Mean Square (NLSM) adaptive filter. The results are experimentally verified under 25%, 50%, 75%, 100% load conditions.

Keywords: Hilbert envelope analysis, induction motor, multiple faults.

1. Introduction

Induction motors are widely applied in industrial applications such as fans, conveyors, pumps, etc. due to their lower cost, easy maintenance and higher reliability. Induction motors can fail due to thermal stress, vibrations, mechanical forces and alignment problems. These problems may occur simultaneously or consecutively [1, 2].

The distribution of faults in induction motors is approximately presented as 69% bearing, 21% stator winding, 7% rotor faults and 3% as shaft/coupling and other faults [3]. Although the bearing faults have the highest percentage among motor faults, broken rotor bars and eccentricity

Article history: received April 27, 2021; revised July 31, 2021; accepted August 16, 2021; available online October 5, 2021.

faults may eventually result in bearing faults. Therefore, it is important to detect the bearing faults along with broken rotor bars and static eccentricity faults.

Bearings are the most critical parts of induction motors [4]. Only 10% of bearings can reach their L10 life in industrial environment [5]. This may happen due to unqualified maintenance crew and insufficient knowledge, misalignment of motor-load, and simultaneous multiple faults [6]. In order to save bearings, it is important to properly monitor the whole spectrum of fault related characteristic harmonic components of stator current and vibration signals.

During the last decades, detection of single faults of three phase induction motors has been studied extensively. At the same time, only few studies of diagnosis of multiple faults have been reported [7]. Several types of simultaneous faults (broken rotor bars, static eccentricity, and bearing faults) of induction motors may produce characteristic harmonic components at the same frequency (with varying amplitudes). Therefore, the detection of multiple faults is more difficult than the detection of a single fault with *Fourier Transform* (FT) based methods.

Stator current signals, vibration signals, acoustic noise signals, temperature, induced voltage, air gap magnetic flux signals are the most commonly used for the diagnosing of faults in induction motors. *Fast Fourier Transform* (FFT) based methods are commonly used for analysis of stator current and vibration signals [8]. Moreover, portable signal analysers also use FFT based methods to detect faults in induction motors [9–11]. Although FFT is frequently used for the analysis of signals, it has some drawbacks. When the motor load is low, the frequencies of characteristic harmonic components of current signals generated by broken rotor bars are very close to the frequency of fundamental component with low amplitudes (and mostly overshadowed by the fundamental components) [12]. Therefore, FFT based methods are ineffective in detecting characteristic harmonic components through using stator current and vibration signals at lower motor loads [2, 13]. In addition, the application of FFT based methods is limited while analysing non-stationary signals [14]. Therefore, FFT based methods are used along with some other methods such as Wavelet [15], *Multiple Signal Classification* (MUSIC) [16], *Artificial Neural Network* (ANN) [17], and *Artificial Intelligence* (AI) methods [18]. A summary of FFT based methods is presented in Table 1 [19–26].

In this paper an alternative method is proposed to detect simultaneous multiple faults of induction motors by using Hilbert envelope analysis along with a *Normalized Least Mean Square*

Table 1. A summary of FFT based methods for diagnosing induction motor faults.

Reference	Year	Signal analysing method	Fault type(s)	Analysed data
[19]	2019	*Motor Current Signature Analysis* (MCSA) – FFT and MCSA – *Discrete Wavelet Transform* (DWT)	Rolling element bearings	Current
[20]	2019	FFT for feature extraction	Rolling element bearings	Current
[21]	2019	FFT and *Principle Component Analysis* (PCA)	Broken end-ring and broken rotor bars	Current
[22]	2018	FFT, *Hilbert time – time* (HTT) and PCA	Rolling element bearings	Vibration
[23]	2017	FFT and wavelet de-noising	Rolling element bearings	Vibration
[24]	2017	FFT	Broken rotor bars and inner race bearing	Vibration
[25]	2016	FFT	Rolling element bearings	Vibration
[26]	2016	FFT – *Independent Component Analysis* (ICA)	Broken rotor bars and bearings	Current

Metrol. Meas. Syst., Vol. 29 (2022), No. 1, pp. 191–205
DOI: 10.24425/mms.2022.138541

(NLMS) adaptive filter. Both stator current and vibration signals are analysed with the proposed method.

The studied simultaneous faults are analysed for two cases:

Case 1: Static eccentricity, three-broken rotor bars and outer-race bearing faults.

Case 2: Static eccentricity, three-broken rotor bars and inner-race bearing faults.

This paper is organized as follows. Section 1 and 3 briefly present the adaptive filter and Hilbert envelope analysis consecutively. The experimental test-bed and the implementation are presented in Section 4 and 5 respectively. The experimental results of the proposed method are given in Section 6. The paper is concluded with Section 7.

2. NLMS adaptive filter

The proposed method contains an NLMS adaptive filter to increase the accuracy of proposed method. The NLMS adaptive filter is used to eliminate noise in current and vibration signals. The optimization of NLMS filter tap weights is given in (1)

$$w(n+1) = w(n) + \mu(n)e(n)x(n), \tag{1}$$

where $e(n)$ is the error signal [27] (see Fig. 1) Adaptive filter weight coefficients filter are updated by the step size factor (μ_n) at each iteration to minimize the error. The design of the filter is implemented in MATLAB. The optimum filter order and the step size are chosen as 64 and 0.2 respectively to provide an acceptable accuracy and convergence time. The structure of adaptive filter is shown in Fig. 1.

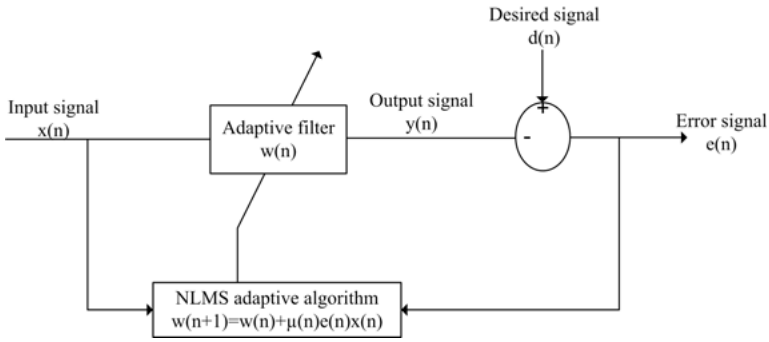

Fig. 1. General structure of the adaptive filter.

3. Hilbert envelope analysis

Hilbert envelope analysis is commonly used in signal processing. The process of the proposed Hilbert envelope analysis consists of four steps. The first step is band pass filtering of stator current and vibration signals to focus on the frequencies of characteristic harmonic components. The second step is the Hilbert transform. The Hilbert transform is widely used to detect the faults in induction motors [2, 22, 28]. Suppose that $x(t)$ is a real time signal, the Hilbert transform of $x(t)$ is given as follows (2)

$$H\{x(t)\} = \frac{1}{\pi t} \cdot x(t). \tag{2}$$

The analytical signal ($z(t)$) can be written as in (3)

$$z(t) = x(t) + jh(t). \tag{3}$$

The third step is envelope analysis. The envelope of $z(t)$ can be calculated as given in (4). The aim of this step is to amplify the amplitude of side-band harmonics

$$E(t) = \sqrt{x^2(t) + h^2(t)}\,. \tag{4}$$

In the last step, the envelope spectrum is observed by performing spectrum analysis to detect the fault related harmonic components.

4. Experimental test-bed

To verify the performance of the proposed method, an experimental test-bed was used. As shown in Fig. 2 the test-bed consists of a 3 kW induction motor, a 5 kVA self-excited synchronous generator, and a 5 kW resistive load. The nameplate of the induction motor used in the experiments is shown in Table 2.

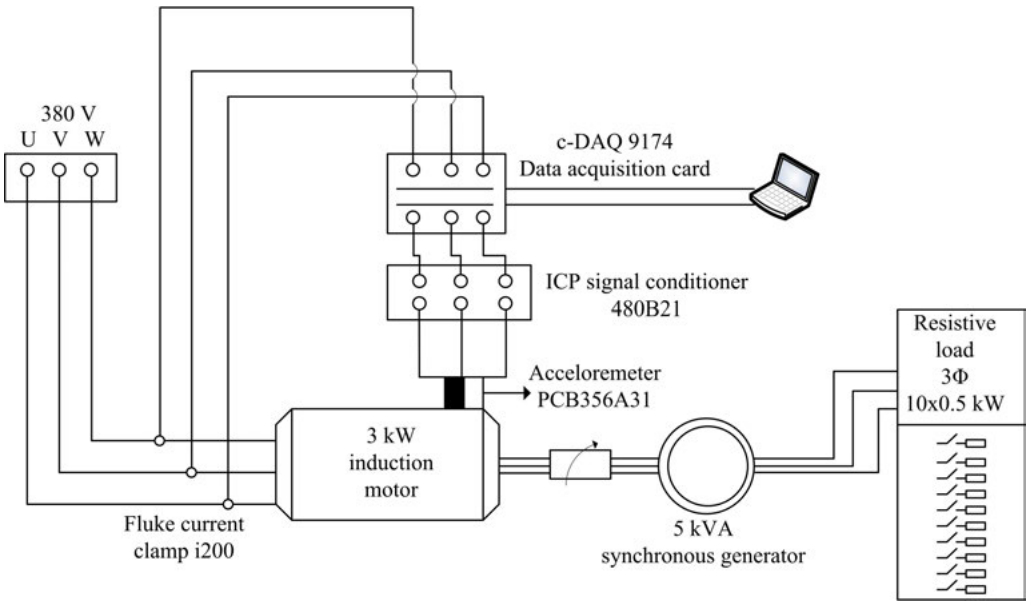

Fig. 2. The experimental test-bed.

Table 2. The nameplate rating of the induction motor.

Phase number	Connection type	Frequency (Hz)	Voltage (V)	Current (A)	Power (W)	Power factor	Speed (rpm)
3	Y	50	380	5.9	3000	0.87	2850

Metrol. Meas. Syst., Vol. 29 (2022), No. 1, pp. 191–205
DOI: 10.24425/mms.2022.138541

Two types of fault scenarios (Case 1 and Case 2), were studied with current and vibration signals under 25%, 50%, 75% and 100% load levels of the induction motor. To create a static eccentricity fault, the bearing housing (Fig. 3a) of the end shield was expanded. A PLA (Polylactic Acid) based bushing, produced with a 3D printer (with static eccentricity), was placed into the bearing housing. Broken rotor bars were emulated by drilling three holes in the rotor bars (See Fig. 3b). 6206.C3 type bearings were used in the induction motor under test. The outer and inner race bearing faults were created by drilling holes on the outer and inner races of bearings respectively as shown in Fig. 3c and Fig. 3d.

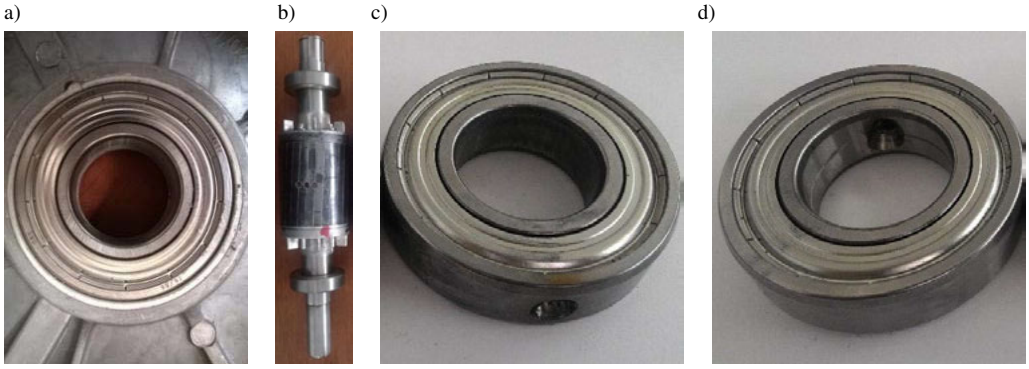

Fig. 3. Induction motor faults: a) static eccentricity fault, b) broken rotor bars, c) outer-race bearing faults, d) inner-race bearing faults.

5. Implementation

Both stator current and vibration signals were recorded at a sampling frequency of 25 kHz with a National Instruments (NI) c-DAQ 9174 data acquisition system (see Table 3). The analyses of the recorded signals were implemented in MATLAB environment. The noise signals are eliminated by the NLMS adaptive filter. Then Hilbert envelope analysis is applied to the filtered signal to detect harmonic components of current and vibration signals. The flowchart of the proposed method is presented in Fig. 4.

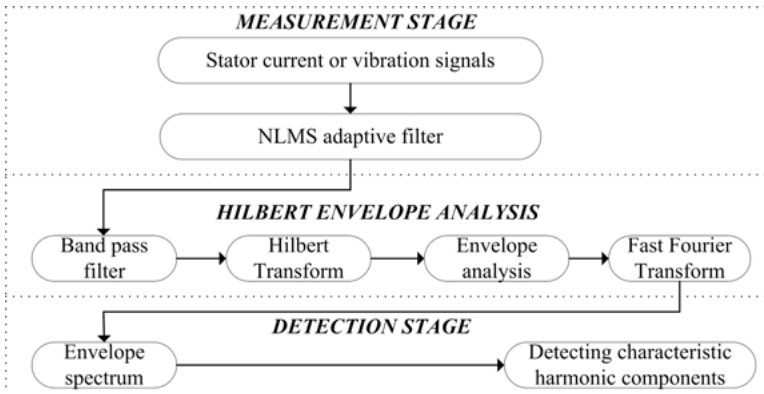

Fig. 4. Flowchart of the proposed method.

Table 3. The specifications of measurement devices.

Type of signals	Measurement device	Amplifier	Data acquisition
Stator current	Fluke i200 AC current clamp	–	NI c-DAQ-9174 with an NI 9225 module
Vibration	Three axis PCB model 356A31	3 channel ICP sensor signal conditioner model 480B21	NI c-DAQ-9174 with an NI 9225 module

6. Results and discussion

A three phase, 3 kW induction motor was used in this study. Two fault cases were studied. In Case 1, static eccentricity, broken rotor bars and outer-race bearing faults were implemented simultaneously. In Case 2, static eccentricity, broken rotor bars and inner-race bearing faults were implemented. At each test case both stator current and vibration signals were recorded.

6.1. Case 1: Static eccentricity, broken rotor bars and outer-race bearing faults

6.1.1. Analysis of stator current signals (Case 1)

The frequencies of characteristic harmonic components of static eccentricity (f_{ecn}) can be calculated using (5) [29]

$$f_{ecn} = f_s \pm k f_r \,, \tag{5}$$

where f_s is the fundamental component of the supply frequency, $k = 1, 2, 3$ and f_r is the rotor (shaft) frequency.

The frequencies of characteristic harmonic components of broken rotor bars (f_{brb}) are as follows (6) [12]

$$f_{brb} = (1 \pm 2ks) \cdot f_s \,, \tag{6}$$

where s is the slip. In the envelope spectrum, the characteristic harmonic component of broken rotor bars is calculated employing $f_s - f_{brb}$ [30].

The frequencies of characteristic harmonic components of bearing faults in the stator current signals are calculated using (7) [31]

$$f_{\text{bear}} = |f_s \pm k \cdot \text{BPFO}| \,, \tag{7}$$

where $k = 2, 3, 4$ and BPFO is Ball Pass Frequency Outer (Outer-Race Failing Frequency).

The frequency of characteristic harmonic components of the outer-race bearing fault is calculated using (8) [31]

$$\text{BPFO} = \frac{N_b}{2} \cdot f_r \cdot \left(1 - \frac{B_d}{P_d} \cdot \cos\varphi\right), \tag{8}$$

where N_b is the number of balls, B_d is the ball diameter and P_d is the pitch diameter, and φ is the ball contact angle. The specifications of the bearing (6206.C3) used in the experiments are given in Table 4.

Table 4. Data sheet of the 6206 bearing [32].

Bearing number	N_b (*Qty*)	B_d (mm)	P_d (mm)	φ (°)
6206	9	9.525	46	0

Metrol. Meas. Syst., Vol. 29 (2022), No. 1, pp. 191–205
DOI: 10.24425/mms.2022.138541

The frequency of characteristic harmonic components of the outer-race bearing fault is calculated in (9)

$$\mathrm{BPFO} = \frac{9}{2} \cdot f_r \cdot \left(1 - \frac{9.525}{46} \cdot \cos 0\right) = 3.57 \cdot f_r \,. \tag{9}$$

The corresponding characteristic harmonic components of current spectra of outer-race bearing faults are presented in Table 5.

Table 5. Current spectra of characteristic harmonic components of outer-race bearing faults.

Load level (%)	**Ball pass frequency of outer-race (Hz)**	**2nd current spectra harmonic (Hz)**	**3rd current spectra harmonic (Hz)**	**4th current spectra harmonic (Hz)**
25	177.2	304	482	659
50	175.0	300	475	650
75	172.9	296	469	642
100	170.6	291	462	632

The results of the proposed method applied to the current signals for Case 1 are shown in Table 6 and Fig. 5.

Table 6. The frequencies of characteristic harmonic components of current analysis for Case 1.

Load level (%)	f_r **(Hz)**	**Broken rotor bars harmonic frequency (Hz)**	**1st harmonic component of static eccentricity (Hz)**	**Outer-race bearing fault 2nd harmonic component (Hz)**
25	49.5	0.954	99.50	304
50	48.9	2.193	98.95	300
75	48.3	3.386	98.56	296
100	47.7	4.721	97.22	291

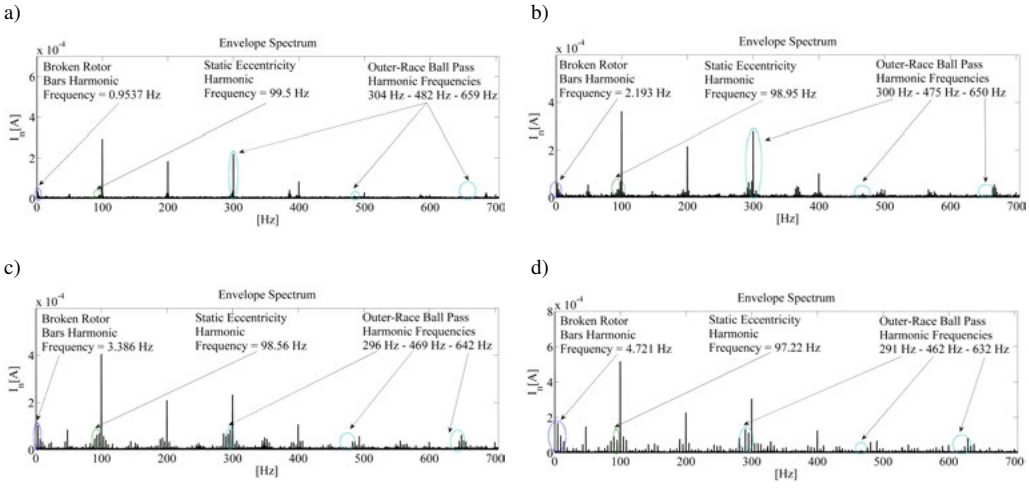

Fig. 5. Characteristic harmonic components of current signal under a) 25% load, b) 50% load, c) 75% load, d) 100% load level of the induction motor.

I_n represents the amplitudes of normalized stator current signals in all figures. In the FFT method, the characteristic harmonic components are detected in pairs as side-bands of the fundamental component. While using the proposed method, the characteristic harmonic components are detected without observing the fundamental component when multiple faults are present. The low-amplitude characteristic harmonic components of broken rotor bars are shifted to 0–10 Hz in the envelope spectrum. Therefore, the proposed method offers an effective solution for problems of overshadowing in dominant harmonic components as presented in Fig. 6. Moreover, the characteristic harmonic components of static eccentricity and outer-race bearing faults are successfully detected with the proposed method.

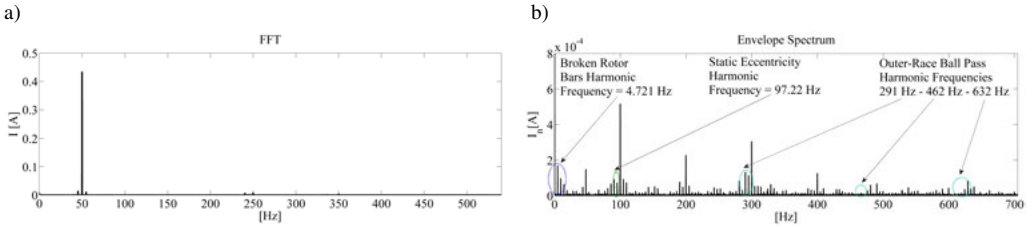

Fig. 6. Analysis of the stator current signal at 100% load level of the induction motor using a) FFT method and b) Hilbert envelope analysis.

6.1.2. Analysis of vibration signals (Case 1)

The static eccentricity fault of the induction motor is detected by comparing the amplitudes of kf_r characteristic harmonic components [33]. If the amplitude of $2f_r$ is greater or equal to $1.5f_r$, the static eccentricity fault is present.

The conventional methods calculate the frequencies of characteristic harmonic components of broken rotor bars (f_{brb}) as in (10) [34], while Hilbert envelope analysis focuses on the $2ksf_s$ harmonic components

$$f_{brb} = f_r \pm 2ksf_s \,. \tag{10}$$

The frequency of characteristic harmonic components of the outer-race bearing fault is calculated as presented in (11)

$$\text{BPFO} = \frac{9}{2} \cdot f_r \cdot \left(1 - \frac{9.525}{46} \cdot \cos 0\right) = 3.57 \cdot f_r \,. \tag{11}$$

The results of the proposed method applied to the vibration signals for Case 1 are presented in Table 7 and Fig. 7.

Table 7. The frequencies of characteristic harmonic components of vibration analysis for Case 1.

Load level (%)	f_r (Hz)	$\frac{\textbf{Amplitude } (2f_r)}{\textbf{Amplitude } (f_r)}$	**Ball pass harmonic frequency of the outer-race (Hz)**	**Broken rotor bars harmonic frequency (Hz)**
25	49.5	1.98	177.2	0.954
50	48.9	1.54	175.0	2.098
75	48.3	1.52	172.9	3.580
100	47.7	1.71	170.6	4.864

Metrol. Meas. Syst., Vol. 29 (2022), No. 1, pp. 191–205
DOI: 10.24425/mms.2022.138541

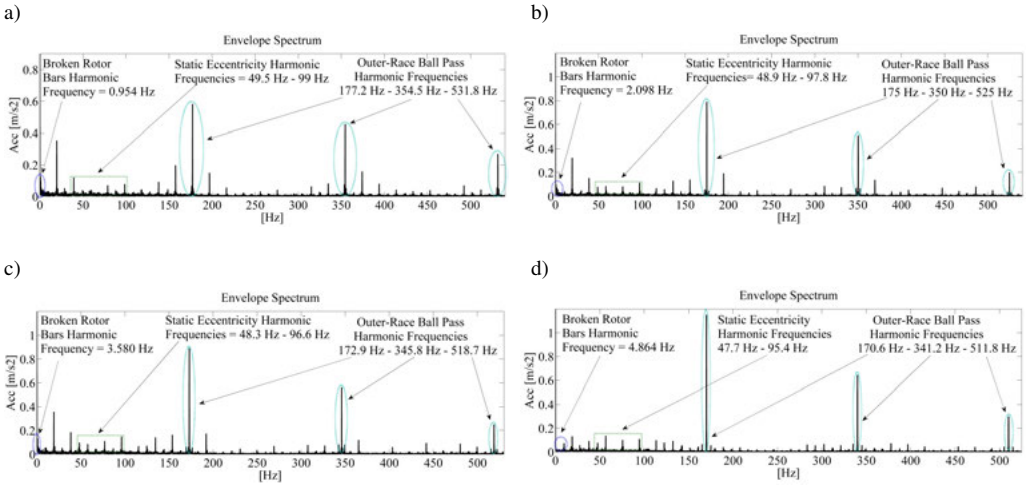

Fig. 7. Characteristic harmonic components of vibration signal under a) 25% load, b) 50% load, c) 75% load, d) 100% load level of the induction motor.

Figure 8 shows that the proposed method is capable of detecting characteristic harmonic components in vibration signals of simultaneous faults at 100% load condition as effectively as the FFT method. The characteristic harmonic components of static eccentricity and outer-race bearing faults are detected successfully (at greater amplitudes) when they are compared to the results of the FFT method. Since the harmonic components of broken rotor bars are shifted to $0 - 10$ Hz frequency region, the proposed method offers an effective solution for problems of overshadowing in dominant harmonic components as presented in Fig. 8.

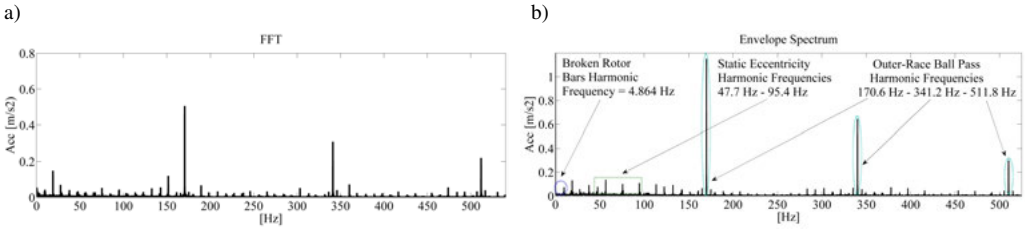

Fig. 8. Analysis of vibration signal at 100% load level of the induction motor using a) FFT method and b) Hilbert envelope analysis.

6.2. Case 2: Static eccentricity, broken rotor bars and inner race bearing faults

6.2.1. Analysis of stator current signals (Case 2)

The frequencies of characteristic harmonic components of the bearing fault obtained by employing stator current signals are calculated as given in (12) [31]

$$f_{\text{bear}} = |f_s \pm k \cdot \text{BPFI}|\,, \tag{12}$$

where $k = 2, 3, 4$ and BPFI is Ball Pass Frequency Inner (Inner-Race Failing Frequency).

The frequency of characteristic harmonic components of the inner-race bearing fault is calculated by (13) [31]

$$\mathrm{BPFI} = \frac{N_b}{2} \cdot f_r \cdot \left(1 + \frac{B_d}{P_d} \cdot \cos\varphi\right). \tag{13}$$

The frequency of characteristic harmonic components of the inner-race bearing fault is calculated in (14)

$$\mathrm{BPFI} = \frac{9}{2} \cdot f_r \cdot \left(1 + \frac{9.525}{46} \cdot \cos 0\right) = 5.43 \cdot f_r \,. \tag{14}$$

The corresponding frequencies of characteristic harmonic components of inner-race bearing faults are presented in Table 8.

Table 8. Current spectra of characteristic harmonic components of inner-race bearing faults.

Load level (%)	**Ball pass frequency of inner-race (Hz)**	**2nd current spectra harmonic (Hz)**	**3rd current spectra harmonic (Hz)**	**4th current spectra harmonic (Hz)**
25	267.4	585	852	1120
50	263.6	577	841	1104
75	260.3	571	831	1091
100	256.6	563	820	1076

The results of the proposed method applied to the current signals for Case 2 are given in Table 9 and Fig. 9.

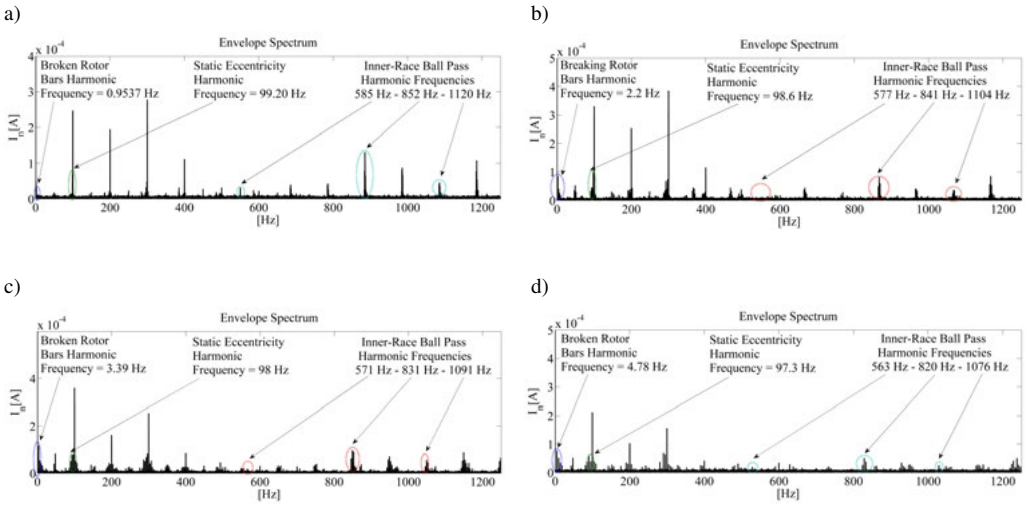

Fig. 9. Characteristic harmonic components of current signal under a) 25% load, b) 50% load, c) 75% load, d) 100% load level of the induction motor.

Figure 10 shows that the proposed method offers an effective solution to the problems of overshadowing in dominant harmonic components in the current signal at 100% load conditions.

Metrol. Meas. Syst., Vol. 29 (2022), No. 1, pp. 191–205
DOI: 10.24425/mms.2022.138541

Table 9. The frequencies of characteristic harmonic components of current analysis for Case 2.

Load level (%)	**f_r (Hz)**	**Broken rotor bars harmonic frequency (Hz)**	**1st harmonic component of static eccentricity (Hz)**	**Inner-race bearing fault 2nd harmonic component (Hz)**
25	49.2	0.954	99.2	585
50	48.6	2.200	98.6	577
75	47.9	3.390	98.0	571
100	47.3	4.780	97.3	563

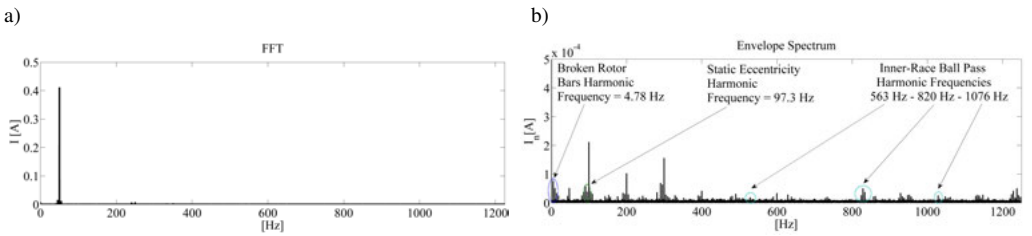

Fig. 10. Analysis of the stator current signal at 100% load level of the induction motor using a) FFT and b) Hilbert envelope analysis.

6.2.2. Analysis of vibration signals (Case 2)

The frequency of the characteristic harmonic components of inner-race bearing fault is calculated as in (15).

$$\text{BPFI} = \frac{9}{2} \cdot f_r \cdot \left(1 + \frac{9.525}{46} \cdot \cos 0\right) = 5.43 \cdot f_r . \tag{15}$$

The results of the proposed method applied to the vibration signals for Case 2 are shown in Table 10 and Fig. 11.

Table 10. The frequencies of characteristic harmonic components of vibration analysis for Case 2.

Load level (%)	**f_r (Hz)**	**$\frac{\text{Amplitude } (2f_r)}{\text{Amplitude } (f_r)}$**	**Ball pass harmonic frequency of the inner-race (Hz)**	**Broken rotor bars harmonic frequency (Hz)**
25	49.5	2.52	267.4	1.001
50	48.6	2.09	263.6	2.289
75	48.0	1.71	260.3	3.529
100	47.3	2.27	256.6	4.721

Figure 12 shows that the proposed method is capable of detecting characteristic harmonic components in vibration signals of simultaneous faults at 100% load condition as effectively as the FFT method.

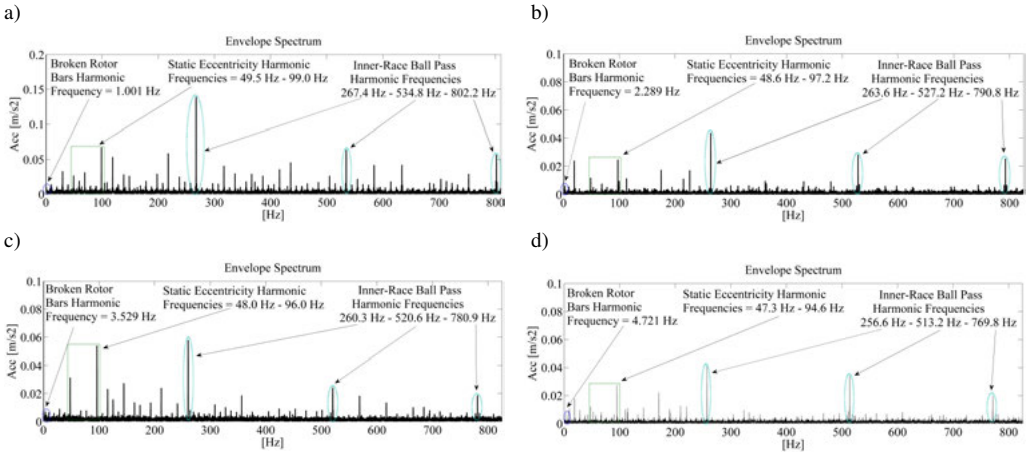

Fig. 11. Harmonic components of vibration signal under a) 25% load, b) 50% load, c) 75% load, d) 100% load level of the induction motor.

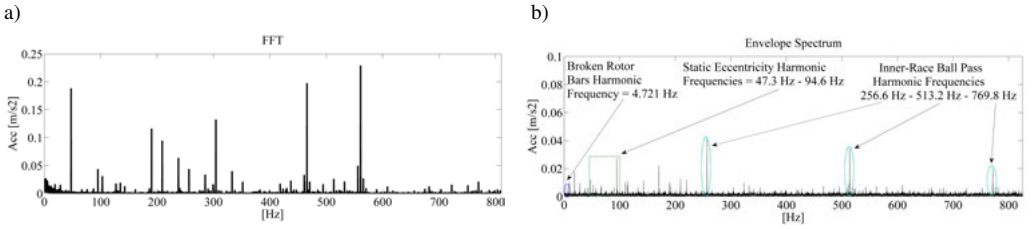

Fig. 12. Analysis of the vibration signals at 100% load level of the induction motor using a) FFT method and b) Hilbert envelope analysis.

7. Conclusions

In this paper, simultaneous multiple faults including static eccentricity, broken rotor bars, outer/inner race bearing faults of a 3 kW induction motor under 25%, 50%, 75% and 100% load levels are investigated by applying Hilbert envelope analysis to the stator current and vibration signals.

The FFT based methods are limited when the motor is lightly loaded with simultaneous faults. The performance of the proposed method has been tested under varying load levels of the induction motor. The results show that the performance of the proposed method is better than the performance of the FFT analysis of the current signals of the induction motor with simultaneous faults at low load levels. It can be seen in Fig. 6 (Case 1) and Fig. 10 (Case 2) that low amplitudes of characteristic harmonic components would not be properly detected by the FFT method (even if the induction motor operates at full load) due to the existence of the dominant fundamental component of characteristic harmonic components.

Although the FFT method offers superior results in the detection of characteristic harmonic components of static eccentricity and bearing faults based on vibration signals, its application is limited in the case of detection of broken rotor bars. The results show that the proposed method successfully detects the characteristic harmonic components of simultaneous broken rotor bars, static eccentricity and outer/inner-race bearing faults at four different load levels of an induction

Metrol. Meas. Syst., Vol. 29 (2022), No. 1, pp. 191–205
DOI: 10.24425/mms.2022.138541

motor by using vibration signals. In addition, the proposed method solves the overshadowing problems of characteristic harmonic components of broken rotor bars and static eccentricity faults of induction motor at low load levels on the part of the dominant fundamental component.

The major contribution of this work is successful detection of low amplitude characteristic harmonic components of simultaneous faults of induction motors.

Acknowledgements

This study was supported by the Scientific and Technological Research Council of Turkey (TUBITAK) with a grant number 116E302.

8. References

References

[1] Tousizadeh, M., Che, H. S., Selvaraj, J., Rahim, N. A., & Ooi, B.-T. (2019). Fault-tolerant field-oriented control of three-phase induction motor based on unified feedforward method. *IEEE Transactions on Power Electronics, 34*(8), 7172–7183. https://www.doi.org/10.1109/TPEL.2018.2884759

[2] Matic, D. & Kanovic, Z. (2017). Vibration based broken bar detection in induction machine for low load conditions. *Advances and Electrical and Computer Engineering, 17*(1), 49–54. https://www.doi.org/10.4316/AECE.2017.01007

[3] Liang, X., Ali, M. Z., & Zhang, H. (2020). Induction motors fault diagnosis using finite element method: A review. *IEEE Transactions on Industry Applications, 56*(2), 1205–1217. https://www.doi.org/10.1109/TIA.2019.2958908

[4] Jiang, Q., Chang, F. & Sheng, B. (2019). Bearing fault classification based on convolutional neural network in noise environment. *IEEE Access, 7*, 69795–69807. https://www.doi.org/10.1109/ACCESS.2019.2919126

[5] Peeters, C., Guillaume, P. & Helsen, J. (2018). Vibration-based bearing fault detection for operations and maintenance cost reduction in wind energy. *Renewable Energy, 116*, 74–87. https://www.doi.org/10.1016/j.renene.2017.01.056

[6] Ünsal, A. (2020). Investigation of parallel misalignment faults of induction motor by using entropy analysis. *Journal of Polytechnic, 23*(4), 1037–1050. https://www.doi.org/10.2339/politeknik.551490

[7] Saucedo-Dorantes, J. J., Delgado-Prieto, M., Ortega-Redondo, J. A., Osornio-Rios, R. A. & Romero-Troncoso, R. d. J. (2016). Multiple-fault detection methodology based on vibration and current analysis applied to bearings in induction motors and gearboxes on the kinematic chain. *Shock and Vibration*, 2016, 1–13. https://www.doi.org/10.1155/2016/5467643

[8] Toliyat, H. A., Nandi, S., Choi, S. & Meshgin-Kelk, H. (2013). *Electric machines, modeling, condition monitoring, and fault diagnosis* (p. 99). CRC Press.

[9] NPP KOHTECT. (29.04.2021). *Vibration Analyzer Data Collector 107VF*. http://www.koh-tect.com/data/products/413822819605767497f351.pdf

[10] RECOVIB®. (29.04.2021). *RECOVIB FEEL 3-Axis Shock & Vibration Smart Probe*. https://micromega-dynamics.com/wp-content/uploads/2020/01/Recovib_FEEL_EN-Rev1p0.pdf

[11] ERBESSD INSTRUMENT®. (07 Nov. 2021). *DigivibeMX®Vibration Analyzer, Data Collector&Dynamic Balancer*. https://www.instrumart.com/assets/DigivibeMX-M30-Datasheet.pdf

[12] Günal, S., Ece D. G. & Gerek Ö. N. (2009). Induction machine condition monitoring using notch-filtered motor current. *Mechanical Systems and Signal Processing, 23*, 2658–2670. https://www.doi.org/ 10.1016/j.ymssp.2009.05.011

[13] Unsal, A. & Kabul, A. (2016). Detection of the broken rotor bars of squirrel-cage induction motors based on normalized least mean square filter and Hilbert envelope analysis. *Electrical Engineering, 98*(3), 245–256. https://doi.org/10.1007/s00202-016-0366-5

[14] Romero-Troncoso, R. d. J. (2016). Multirate signal processing to improve FFT-based analysis for detecting faults in induction motors. *IEEE Transactions on Industrial Informatics, 13*(3), 1291–1300. https://www.doi.org/10.1109/TII.2016.2603968

[15] Liu, M. & Weng, P. Y. (2019). Fault diagnosis of ball bearing elements: A generic procedure based on time-frequency analysis. *Measurement Science Review, 19*(4), 185–194. https://www.doi.org/10.2478/msr-2019-0024

[16] Elbouchikhi, E., Choqueuse, V. & Benbouzid, M. (2016). Induction machine bearing faults detection based on a multi-dimensional MUSIC algorithm and maximum likelihood estimation. *ISA Transactions, 63*, 413–424. https://www.doi.org/10.1016/j.isatra.2016.03.007

[17] Chen, Z., Deng, S., Chen, X., Sanchez, R.-V. & Quin, H. (2017). Deep neural networks-based rolling bearing fault diagnosis. *Microelectronics Reliability, 75*, 327–333. https://www.doi.org/10.1016/j.microrel.2017.03.006

[18] Unal, M., Onat, M., Demetgul, M. & Kucuk, H. (2014). Fault diagnosis of rolling bearings using a genetic algorithm optimized neural network. *Measurement, 58*, 187–196. https://www.doi.org/10.1016/j.measurement.2014.08.041

[19] Bessous, N., Sbaa, S. & Megherbi, A. C. (2019). Mechanical fault detection in rotating electrical machines using MCSA-FFT and MCSA-DWT techniques. *Bulletin of the Polish Academy of Sciences: Technical Sciences, Vol 67*(3), 571–582. https://www.doi.org/10.24425/bpasts.2019.129655

[20] Pandarakone, S. E., Mizuno Y. & Nakamura H. (2019). A comparative study between machine learning algorithm and artificial intelligence neural network in detecting minor bearing fault of induction motors. *Energies, 12*(11), 2105. https://doi.org/10.3390/en12112105

[21] Yoo Y. J. (2019). Fault detection of induction motor using Fast Fourier Transform with feature selection via Principal Component Analysis. *International Journal of Precision Engineering and Manufacturing, 20*, 1543–1552. https://www.doi.org/10.1007/s12541-019-00176-z

[22] Pang, B., Tang, G., Tian, T. & Zhou, C. (2018). Rolling bearing fault diagnosis based on improved HTT transform. *Sensors, 18*(4), 1203. https://www.doi.org/10.3390/s18041203

[23] Mishra, C., Samantaray, A. K. & Chakraborty, G. (2017). Rolling element bearing fault diagnosis under slow speed operation using wavelet de-noising. *Measurement, 103*, 77–86. https://www.doi.org/10.1016/j.measurement.2017.02.033

[24] Naha, A., Thammayyabbabu, K. R., Samanta, A. K., Routray, A. & Deb, A. K. (2017). Mobile application to detect induction motor faults. *IEEE Embedded Systems Letters, 9*(4), 117–120. https://www.doi.org/10.1109/LES.2017.2734798

[25] Maruthi, G. S. & Hegde, V. (2016). Application of MEMS accelerometer for detection and diagnosis of multiple faults in the roller element bearings of three phase induction motor. *IEEE Sensors Journal, 16*(1), 145–152. https://www.doi.org/10.1109/JSEN.2015.2476561

[26] Yang, T., Pen, H., Wang, Z. & Chang, C. S. (2016). Feature knowledge based fault detection of induction motors through the analysis of stator current data. *IEEE Transactions on Instrumentation and Measurement, 65*(3), 549–558. https://www.doi.org/10.1109/TIM.2015.2498978

[27] Yu, Z., Cai, Y. & Mo, D. (2020). Comparative study on noise reduction effect of fiber optic hydrophone based on LMS and NLMS algorithm. *Sensors, Vol 20*(1), 301. https://www.doi.org/10.3390/ s20010301

Metrol. Meas. Syst., Vol. 29 (2022), No. 1, pp. 191–205
DOI: 10.24425/mms.2022.138541

[28] Kabul, A. & Ünsal, A. (2021). An alternative approach for the detection of broken rotor bars and bearing faults of induction motor based on vibration signals. *Proceedings of the 8th International Conference on Electrical and Electronics Engineering (ICEEE)*, Turkey, 126–131. https://www.doi.org/10.1109/ICEEE52452.2021.9415920

[29] Faiz, J. & Moosavi S. M. M. (2016). Eccentricity fault detection – From induction machines to DFIG – A review. *Renewable and Sustainable Energy Reviews, 55*, 169–179. https://www.doi.org/10.1016/j.rser.2015.10.113

[30] Kabul, A. & Ünsal, A. (2021). Detection of broken rotor bars of induction motors based on the combination of Hilbert envelope analysis and Shannon entropy. *tm – Technisches Messen, 88*(1), 45–58. https://www.doi.org/10.1515/teme-2020-0066

[31] Boudinar, A. H., Benouzza, N., Bendiabdellah, A. & Khodja, M.-E.-A. (2016). Induction motor bearing fault analysis using a Root-MUSIC method. *IEEE Transactions on Industry Applications, 52*(5), 3851–3860. https://www.doi.org/10.1109/TIA.2016.2581143

[32] GBMN Bearing USA Ltd. (29.04.2021). *Data Sheet of 6206 Bearing*. https://www.gmnbt.com/catalog/product/bb-6206-radial-ball-bearing/

[33] Hujare, D. P. & Karnik, M. G. (2018). Vibration responses of parallel misalignment in Al shaft rotor bearing system with rigid coupling. *Materials Today: Proceedings, 5*(11), 23863-23871. https://www.doi.org/10.1016/j.matpr.2018.10.178

[34] Wang, Z., Yang, J., Li, H., Zhen, D., Xu Y. & Gu, F. (2019). Fault identification of broken rotor bars in induction motors using an improved cyclic modulation spectral analysis. *Energies, 12*(17), 3279. https://www.doi.org/10.3390/en12173279

Ahmet Kabul received his B.Sc. in electrical-electronic engineering from Anadolu University, Eskisehir, Turkey, in 2009; and his M.Sc. in electrical-electronic engineering from Dumlupinar University, Kutahya, Turkey, in 2013. He is currently pursuing the Ph.D. degree in electrical-electronic engineering at Kutahya Dumlupinar University. From 2009 to 2018, he worked as a research assistant at Dumlupinar University. From March 2018 to May 2019, he worked in a textile factory as a maintenance engineer. From May 2019 to present, he has been with the Department of Electrical-Electronic Engineering of Burdur Mehmet Akif Ersoy University as a research assistant. His research interests include diagnosing of induction motor failures.

Abdurrahman Ünsal received his B.Sc. from Gazi University (Ankara/Turkey) in 1992, his M.Sc. degree from Oklahoma State University (USA) in 1996, and his Ph.D. degree from Oregon State University (USA) in 2001. He is currently working as a Professor at the Department of Electrical and Electronic Engineering of Kutahya Dumlupinar University in Turkey. His research interests are power quality, fault detection and control of electrical machines, renewable energy, and smart grids. He has been an IEEE member since 2000.